

Ground states versus low-temperature equilibria in random field Ising chains

G. SCHRÖDER^{1,2}, T. KNETTER^{1,2}, M. J. ALAVA³ and H. RIEGER⁴

¹ *Institut für Theoretische Physik, Universität zu Köln, 50926 Köln, Germany*

² *NIC c/o Forschungszentrum Jülich, 52425 Jülich, Germany*

³ *Helsinki University of Techn., Lab. of Physics, P.O.Box 1100, 02015 HUT, Finland*

⁴ *Theoretische Physik, Universität des Saarlandes, 66041 Saarbrücken, Germany*

PACS. 05.40.-a – Fluctuation phenomena, random processes, noise, and Brownian motion.

PACS. 05.50+q – Lattice theory and statistics (Ising, Potts, etc.).

PACS. 75.50.Lk – Spin glasses and other random magnets.

Abstract. – We discuss with the aid of random walk arguments and exact numerical computations the magnetization properties of one-dimensional random field chains. The ground state structure is explained in terms of absorbing and non-absorbing random walk excursions. At low temperatures, the magnetization profiles follow those of the ground states except at regions where a local random field fluctuation makes thermal excitations feasible. This follows also from the non-absorbing random walks, and implies that the magnetization length scale is a product of these two scales. It is not simply given by the Imry-Ma-like ground state domain size nor by the scale of the thermal excitations.

In statistical mechanics of random systems the search for universality can be interpreted geometrically. That is, if the introduction of disorder into a system is relevant, the real-space properties of the physical states can be understood in terms of scaling exponents. These describe the fluctuations of a domain wall, or the behavior of a spin-spin correlation function. The central ingredient is that the configurational energy is coupled to geometric fluctuations. Consider a domain wall in a magnet. If the spatial fluctuations are described by a roughness exponent ζ , then there is an associated exponent θ describing the free or ground state energy fluctuations. Assuming that the 'zero temperature fixed point' scenario is true or that the entropy is irrelevant at low enough temperatures, this is all what is needed to describe the physics. The system evolves via Arrhenius-like dynamics so that the cost of moving in the energy landscape is given by the usual exponential factor $\exp(\Delta E \beta)$, where $\beta = 1/T$ and T is the temperature, and $\Delta E \sim l^\zeta$ relates the cost to the scale length of the perturbation l .

Consider now a random magnet. It has a ground state (GS) which is described exactly by the positions and arrangement of the domain walls. Examples abound in particular in Ising systems, where non-trivial GSs exist for spin glasses and random field systems [1]. In this work we investigate with random walk arguments and exact numerical computations how the aforementioned picture applies in the case of one-dimensional random field chains. We find that for arbitrary field distributions [2] the GS structure can be understood via the

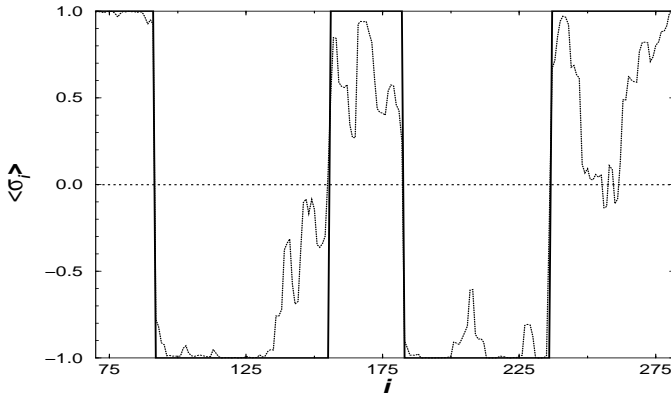


Fig. 1 – Example for a ground state configuration (bold line) of a chain segment for a particular realization of random fields as compared to the equilibrium expectation values of the local magnetization $\langle \sigma_i \rangle$ at temperature $T = 0.45J$. In the leftmost domain nearly no melting occurs, the region right of $i = 125$ is a typical example for boundary melting and in the rightmost domain the bulk melting is so strong that even magnetization reversal occurs.

random walk picture, which is compared to exact numerical GS computations. At finite temperatures we resort to scaling arguments based on this random walk picture, and again to an exact numerical determination of the magnetization. This allows us to make conclusions about the behavior in the same sample in both cases. Our main finding is, in addition to recovering the GS from the random walk picture, the emergence of two relevant length scales. These arise from the zero-temperature length scale of the domains and the typical size of ‘easy’ excitations at a given temperature. The latter changes the correlation length of the magnetization, and thus leads to the fact that in our case the low-temperature physics is characterized not only by the zero-temperature scaling. The 1d RFIM has received recently attention [3] since it is simple enough that decimation-type real space renormalization can be applied to domain wall dynamics (each DW undergoes logarithmic Sinai diffusion [4]), which can be compared with our findings concerning the asymptotic state of such processes. The zeroes of the magnetization profile simply denote the equilibrium positions of domain walls at $T > 0$, and the extra physics consists of additional domain walls added to the GS structure. The chain is also the simplest example of a random magnet with a competition of non-trivial GS and thermal excitations (e.g. random bond Ising magnets have a trivial GS).

In the following we investigate the Hamiltonian

$$H = - \sum_{i=1}^N J \sigma_i \sigma_{i+1} + \sum_i h_i \sigma_i \quad (1)$$

where the σ ’s are spins located at sites i of the chain, and h_i are random fields picked from a suitable probability distribution $P(h_i)$ with zero mean and variance h_r . For a binary distribution $h_i = \pm h_{i,r}$ the model is equivalent to a spin glass chain (with couplings $J_i = \pm J$) in a homogeneous external field h_r [5,6]. Fig. 1 shows typical GS and finite temperature ($T = 0.4$) magnetization profiles obtained from the numerical procedures described below. The GS domain size is often thought to be given by the Imry-Ma argument [7], which states that the domain field energy balances the cost from the domain walls on a scale $[l]_{\text{av}} \sim 1/h_r^2$ in 1D and $[\dots]_{\text{av}}$ denotes the disorder average. This reasoning omits the global optimization behind the

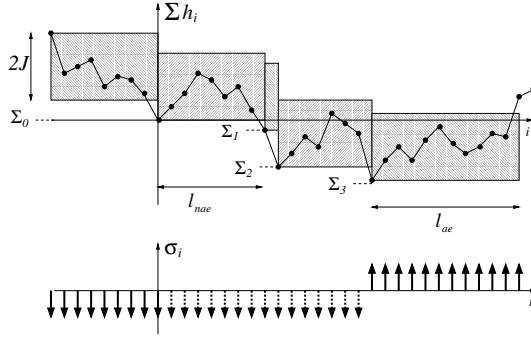


Fig. 2 – Terminology used for the description of the RW arguments. For further details see text.

GS; later we discuss the exact way the optimization becomes visible in. At finite but small temperatures the magnetization changes due to two reasons. The GS domain walls fluctuate, and thus the $m(x)$ -profile is smoothed out around the GS positions. More interestingly, there are regions inside domains where the magnetization can even undergo a local reversal. Both of the cases arise from the local random field configurations as we now demonstrate.

The starting point for the random walk argument is the fact that any sequence \mathcal{S} of lattice sites i with $|\sum_{i \in \mathcal{S}} h_i| \geq 2J$ evidently leads to a GS spin structure with $\sigma_i = +1 \quad \forall i \in \mathcal{S}$ if $\sum_{i \in \mathcal{S}} h_i \geq 2J$ (and $\sigma_i = -1 \quad \forall i \in \mathcal{S}$ if $\sum_{i \in \mathcal{S}} h_i \leq -2J$) independent of the local fields h_j at sites $j \notin \mathcal{S}$. The system can thus be split up into such *absorbing excursions* and into the remaining lattice sites, which make up so-called *non-absorbing excursions*.

Fig. 2 illustrates these concepts. An *absorbing excursion* is a sequence of spins starting at some lattice site i and ending at the lattice site $j \geq i$, with the field-sum $|\sum_{i \in \mathcal{S}} h_i|$ for the first time becoming greater or equal to $2J$:

$$\left| \sum_{l=i}^j h_l \right| \geq 2J \quad \text{and} \quad \left| \sum_{l=i}^k h_l \right| < 2J \quad \forall i < k < j. \quad (2)$$

In Fig. 2 the left- and rightmost sequences are absorbing excursions, of length l_{ae} . A sequence \mathcal{S}' of spins from i to $j \geq i$ is a *non-absorbing excursion* if

$$\bar{\sigma} \sum_{l=i}^j h_l \leq 0 \quad \text{and} \quad 0 < \bar{\sigma} \sum_{l=i}^k h_l < 2J \quad \forall i < k < j \quad (3)$$

where $\bar{\sigma} = \pm 1$ is the orientation of the spins within the preceding absorbing excursion. The length of a non-absorbing excursion is l_{nae} . A simple 'step down' (like from Σ_1 to Σ_2) is included in this definition.

The GS now follows as a sequence of absorbing and non-absorbing excursions. It, and the Zeeman energy and mean domain-length can be determined with the three rules: (1) determine an absorbing excursion \mathcal{S}_0 for a given field configuration. If it starts at site i_0 , ends at j_0 , and $\bar{\sigma}$ is the sign of its field-sum, then $\sigma_k = \bar{\sigma}$ for all $k \in \mathcal{S}_0$. (2) start from $j_0 + 1$ and find all n_{nae} of non-absorbing excursions until the next absorbing excursion \mathcal{S}_1 (from i_1 to j_1) is found, whose field-sum is by definition opposite in sign to the preceding one. The sites k belonging to the non-absorbing excursions have the same orientation $\sigma_k = \bar{\sigma}$ as those within \mathcal{S}_0 . The orientation of the spins at sites l within \mathcal{S}_1 is opposite to the latter one, $\sigma_l = -\bar{\sigma}$. (3) starting again at $j_1 + 1$ the search (2) for the next absorbing excursion then leads to

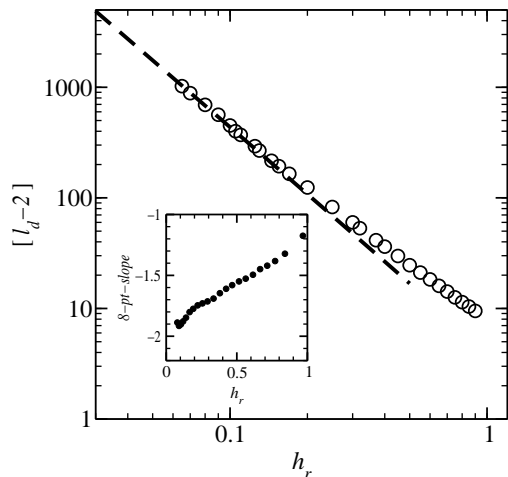


Fig. 3

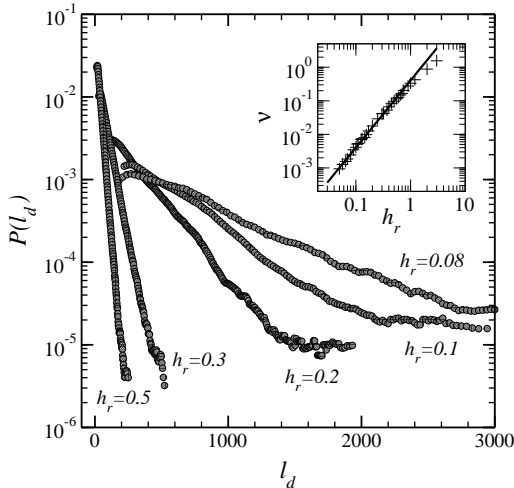


Fig. 4

Fig. 3 – Average domain length as a function of h_r . The dotted line is a fit to eq. (5) with $a = -0.74$, $b = 0.25$ and $c = 1.4$. The inset shows the 8-point slope of the presented data again yielding an exponent 2 in the limit of small field amplitudes.

Fig. 4 – Probability distribution of the domain lengths l_d . Apart from a non-exponential tail which might be due to finite size effects the decay is exponential with decay rate ν . **Inset:** The decay rate ν as a function of h_r . For $h_r \ll 1$ the data are compatible with $\nu \sim h_r^2$ (bold line).

the overall GS. These steps actually define a fast algorithm for finding the GS, though for historical reasons we have used the mapping to the max-flow/min-cut problem [1].

The mean domain length $[l_d]_{av}$ is given by

$$[l_d]_{av}(h_r) = [n_{nae}]_{av}[l_{nae}]_{av} + [l_{ae}]_{av}. \quad (4)$$

Thus the domain length consists of two distinct contributions and we need to estimate the h_r -dependence of $[n_{nae}]_{av}$, $[l_{nae}]_{av}$ and $[l_{ae}]_{av}$. The fieldsum over the local fields of a non-absorbing excursion is a RW with absorbing boundaries at $\sum_{nae} h_i = 0$ and $\sum_{nae} h_i = 2J$ and random step size with zero mean and variance h_r . Rescaling the step size $h'_i = h_i/h_r \rightarrow 1$ this becomes a 1d RW starting from $x = 1$ at $t = 0$ with random step lengths with mean zero and variance one (for a binary distribution $h_i = \pm h_r$ it yields a conventional lattice random walk with $h'_i = \pm 1$) and absorbing boundaries at $x = 0$ and $x = L = 2J/h_r$. The probability $P_0(t, L)$ to be absorbed at $x = 0$ within the time interval $[t, t + dt]$ without having been absorbed at $x = L$ reads [8] $P_0(t, L) \propto t^{-3/2}$ for $1 \lesssim t \lesssim L^2$ and decays exponentially for $t \gtrsim L^2$. Integration over $P_0(t, L)$ leads to $[l_{nae}]_{av} \sim L \propto h_r^{-1}$. The mean number $[n_{nae}]_{av}$ of consecutive non-absorbing excursions follows due to the fact that the probability for an excursion to be absorbing grows as $p_{ae} \sim 1/L \propto h_r$ [9]. Thus $P(n_{nae}) \sim (1 - p_{ae})^{n_{nae}}$ decays exponentially. As a consequence $n_{nae} \sim 1/\ln(1 - p_{ae})$ and the mean length of an absorbing excursion grows like h_r^{-2} . Finally eq. (4) reads

$$[l_d]_{av}(h_r) \sim \frac{a}{h_r \ln(1 - b h_r)} + \frac{c}{h_r^2} \rightarrow \frac{e}{h_r^2} \quad \text{for } h_r \rightarrow 0 \quad (5)$$

where one expects $b < 1$, $a < 0$ and $-a \approx c$. Note that $a/h_r \ln(1 - b h_r) \sim h_r^{-2}$ for $h_r \rightarrow 0$

and for $h_r < 0.5$ no significant difference between $a/[h_r \ln(1 - b h_r)]$ and h_r^{-2} can be observed. The asymptotic limit follows the Imry-Ma scaling, though the physics is more complicated.

This result is confirmed by computations of exact ground states. The data was obtained for a Gaussian random field distribution with zero mean and variance h_r and averaged over 10^5 disorder configurations. The system size is large enough ($L = 5000$) such that $[l_d]_{\text{av}} \ll L$ even for the smallest field strength h_r . Fig. 3 shows our numerical result for the average length $[l_d - 2]_{\text{av}}$ of the GS domains as a function of the field amplitude h_r . In the limit $h_r \rightarrow \infty$ $[l_d]_{\text{av}} \rightarrow 2$ since all the spins align with their local fields. In the limit $h_r \ll J$ the data fit well to the predicted form eq. (5), scaling as h_r^{-2} for $h_r \rightarrow 0$. Moreover, as can be seen in Fig. 4 the probability distribution of the domain sizes decays exponentially, with a decay rate ν that scales inversely proportional to $[l_d]_{\text{av}}$, i.e. $\nu(h_r) \propto h_r^2$.

The field energy of a domain can be computed as a function of h_r and l_d by noting that both a single absorbing excursion and all of the non-absorbing excursions contribute. The former contributes a constant ($2J$), depending neither on h_r nor on l_d . Each non-absorbing excursion adds an amount of $\mathcal{O}(h_r)$ so that the sum self-averages. The contribution of a single non-absorbing excursion equals $\Sigma_i - \Sigma_{i-1} \sim h_r$, i.e. the step width of the RW. Thus the field energy results from the number of non-absorbing excursions in a domain, n_{nae} , plus $2J$. From (5) we learn that in the limit $h_r \rightarrow \infty$ the contribution of the absorbing and non-absorbing walks to $[l_d]_{\text{av}}$ scale similarly such that we expect that for a fixed domain size $[n_{nae}(l_d)]_{\text{av}} \propto l_d/[l_{nae}]_{\text{av}} \propto l_d h_r$. Thus

$$[E_f(l_d)]_{\text{av}} = 2J + [n_{nae}(l_d)]_{\text{av}} h_r = 2J + d h_r^2 [l_d]_{\text{av}} \quad (6)$$

The numerics confirms this result: Fig. 5 shows the data for the mean Zeeman energy $[E_f(l_d)]_{\text{av}}$ of domains of length l_d . From the slopes of the straight lines we learn that $[E_f(l_d)]_{\text{av}}$ is linear in the domain length and from the offsets that it grows like h_r^2 , independent of the field distribution $P(h_i)$. Note that from a *naïve* random walk picture one would expect $[E_f(l_d)]_{\text{av}} \propto l_d^{1/2} h_r$, which is incorrect.

We now turn our attention to equilibrium configurations, i.e. the local magnetization $m(x)$ and the domain structure at $T > 0$. Using numerical transfer matrix methods [10,11] to compute the partition function Z_N we can compute the exact expectation value $\langle \sigma_r \rangle$ for each spin σ_r by calculating the product of the N 2×2 transfer matrices. Since some of the random matrix elements can be very small, floating point accuracy gives a lower limit of $T = 0.05$.

First we address the scale-lengths of the equilibrium magnetization by computing the average length $[l_m]_{\text{av}}$ that separates two zeroes of the magnetization $m(x)$. Figure 6 demonstrates how this length-scale changes with temperature, if we first scale away the $T = 0$ -dependence on the field. A further collapse with the right combination of h_r and T makes it possible to observe an universal scaling function for $[l_m]_{\text{av}}$

$$[l_m]_{\text{av}} = [l_d]_{\text{av}} f(T/h_r^{2/3}), \quad (7)$$

where the scaling function $f \rightarrow 1$ with $T \rightarrow 0$. The dependence of $[l_m]_{\text{av}}$ on the combination of temperature and field strength does not follow an Imry-Ma-like scaling but is a consequence of entropic effects. The length $[l_m]_{\text{av}}$ at a finite temperature is determined by both a zero-temperature scale ($[l_m]_{\text{av}}$) and thermal fluctuations. The following argument can explain the scaling variable $h_r^{2/3}/T$, analogously to spin glass chains in an external field [6]. Once again consider the non-absorbing random walks which the domains consist of. Some of these inside a typical domain are such that the random walk sum of fields over the excursion is close to $2J$. These almost-absorbing walks are the sequences (of spins) most likely to be flipped at

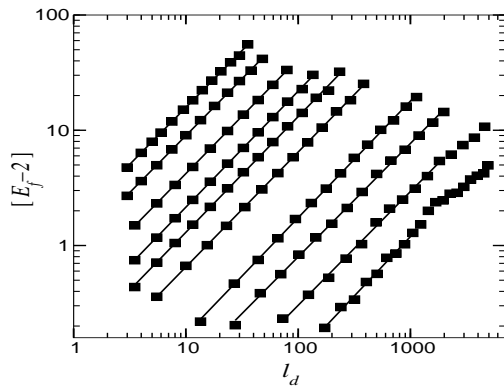


Fig. 5

Fig. 5 – Mean Zeeman energy $H_Z - 2J$ corresponding to a particular domain length l_d in a log-log plot. $h_r = 3.0, 2.0, 1.2, 1.0, 0.8, 0.6, 0.4, 0.2, 0.13, 0.08, 0.05$ from top to bottom. The slopes of the straight lines are all within the interval 1.00 ± 0.05 . The data are averaged over 10^5 disorder configurations. The straight lines represent least square fits.

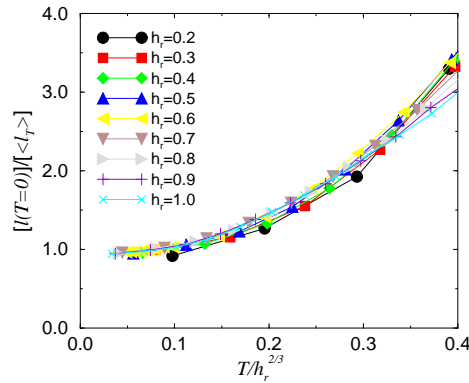


Fig. 6

Fig. 6 – Scaling-plot for the average domain-lengths at finite temperatures: $[l(T=0)]_{av} / [l_T]$ versus $T/\xi(h)$ for different values of the field strength h_r , where the length scale $\xi(h) \propto h_r^{2/3}$.

finite temperatures. The cost of flipping such a part of a domain is proportional to J , which if measured in terms of h_r can be written with the help of the length-scale l of the non-absorbing excursions, $h_r \sim 1/l$. This is *almost* equal to the Zeeman-energy optimized over the excursion, which scales as $E_f \sim h_r l^{1/2}$. Equating the cost with the gain and solving for the energy scale (E_f) as a function of field gives rise to the Arrhenius factor $E_f/T \sim h_r^{2/3}/T$.

As Fig. 1 demonstrates, the magnetization profile at $T > 0$ differs from the GS due to domain wall fluctuations *and* internal cluster reversals. To study this quantitatively we introduce a parameter $c \in (0, 2)$ and define a reversal to be a sequence of spins for which $|\langle \sigma_i \rangle(T) - \sigma_i(T=0)| > c$ holds; moreover the definition can be applied to both processes separately revealing interesting details. Since bulk reversal is always coupled with the breaking of two extra bonds one expects that domain wall fluctuations dominate. However, the former contributes a considerable portion to the total melting even at low temperatures (Fig. 7). The relative portion of bulk reversals at first grows with temperature for all values of c since the gain in entropy allows for more broken bonds. Moving the threshold c away from 1 and -1 respectively, a greater number of bulk segments are identified. Eventually for very large c even more bulk than boundary reversals are observed. The characteristic reversal rates are different for the two processes, and related via the empirical formula

$$\left(\frac{\Delta m}{\Delta T}\right)_{bulk} = \alpha \left(\frac{\Delta m}{\Delta T}\right)_{bound}, \quad (8)$$

with $\alpha \approx 1.63$. Thus the change in magnetization with increasing T is stronger inside the GS domains than at their boundaries. These results are independent of the field strength.

In conclusion, we have studied the magnetization properties of one-dimensional RFIM chains. These can be explained using of random walk arguments. While the GS structure is found to be a sequence of absorbing and non-absorbing excursions, the finite-temperature

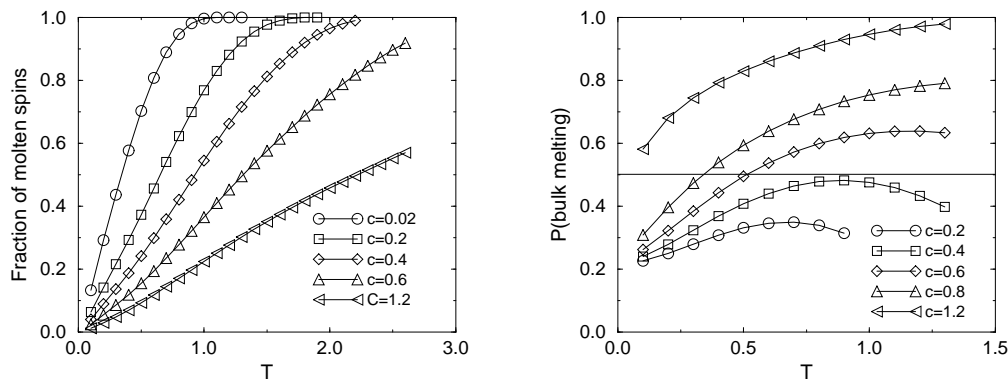


Fig. 7 – **Left:** Fraction of melted spins as a function of temperature for different values of c . **Right:** Portion of those spins is displayed which reside inside bulk segments. $L = 400$, $h_r = 1.0$.

magnetization is complicated by thermal excitations. These are explained with the help of almost-non-absorbing walks. The results illustrate how a global optimization problem influences physics at $T > 0$ in systems where the geometric arrangement of domain walls is crucial. Yet, extending the results to higher dimensions seems insolvable.

* * *

This work has been supported by the Academy of Finland and the German Academic Exchange Service (DAAD) within a common exchange project, and separately, by the A. of F.'s Center of Excellence Program.

REFERENCES

- [1] H. Rieger, *Frustrated Systems: Ground State Properties via Combinatorial Optimization*, Lecture Notes in Physics **501**, p.122 (Springer Verlag Heidelberg, 1998); M. Alava, P. Duxbury, C. Moukarzel and H. Rieger, *Combinatorial optimization and disordered systems*, in: "Phase Transition and Critical Phenomena" vol. **18** (ed. C. Domb and J. L. Lebowitz), p.141 (Academic Press, Cambridge, 2000).
- [2] See J.M. Luck, M. Funke, and T.M. Nieuwenhuizen, J. Phys. **A24**, 4155 (1991), and references therein for (complicated) analytical treatments of specific field distributions.
- [3] D. S. Fisher, P. LeDoussal, and C. Monthus, Phys. Rev. Lett. **80**, 3539 (1998).
- [4] For a review on anomalous and Sinai diffusion see J. P. Bouchaud and A. Georges, Phys. Rep. **195**, 127 (1990).
- [5] M. Puma and J. F. Fernandez, Phys. Rev. B **18**, 1391 (1978); U. Brandt and W. Gross, Z. Phys. B **31**, 237 (1978); B. Derrida, J. Vannimenus, and Y. Pomeau, J. Phys. C **11**, 4749 (1978).
- [6] H.-H. Chen and S. K. Ma, J. Stat. Phys. **29**, 717 (1982).
- [7] Y. Imry and S.-K. Ma, Phys. Rev. Lett. **35**, 1399 (1975).
- [8] For a similar example see appendix of F. Iglói and H. Rieger, Phys. Rev. B **57**, 11404 (1998).
- [9] H. Rieger and F. Iglói, Europhys. Lett. **45**, 673 (1999).
- [10] R. Bruinsma and G. Áplli, Phys. Rev. Lett. **50**, 1494 (1983).
- [11] A. Crisanti, G. Paladin, A. Vulpiani, *Products of Random Matrices in Statistical Physics*, Springer Series in Solid-State Sciences **104**, (Springer-Verlag, Heidelberg, 1993)